Supporting Information

Cicero et al. 10.1073/pnas.0901596106

SI Text

In addition to these detailed materials and methods, specific protocols can be found at: http://www.stjude.org/dyer or in publications cited herein.

Antibodies, Immunostaining, and [^{3}H]-thymidine Labeling. For the immunostaining of retinal tissues, we fixed the fresh retinae with 4% PFA for 1 day and embedded them into 4% agarose. We made 50-μm sections by a vibratome (Leica VT1000S) or 15-μm cryosections by cryostat (Leica CM3050S) and stained them with the antibodies as described in ref. 1. For the immunostaining of dissociated cells, we used trypsin, and DNase I for the dissociation as described in ref. 2. For immunostaining of the CE-differentiation cultures, we used the antibody dilution for dissociated cells as shown in the table above. To label the S-phase cells, we cultured the retinal explants for 4 or 24 h with [^{3}H]-thy (5 μCi/mL; 89 μCi/mmol). Autoradiography was carried out as described in ref. 2. Toluidine blue staining of plastic sections was described in ref. 3.

Real Time RT-PCR. Real time RT-PCR experiments were performed using the ABI 7900 HT Sequence Detection System (Applied Biosystems). Primers and probes were designed using Primer Express software (Applied Biosystems). Taqman probes were synthesized with 5′-FAM and 3′-BHQ. RNA was prepared using TRIzol and cDNA was synthesized using the SuperScript system (Invitrogen). Samples were analyzed in duplicate and normalized to *Gapdh* and *Gpi1* expression levels.

Electron Microscopy, 3D Reconstruction, and Dual Beam FIB. For electron microscopy (EM), animals were anesthetized with avertin until a loss of deep tendon reflexes. Transcardial perfusion was performed with carboxygenated Ames medium supplemented with 40-mM glucose to clear the vasculature, followed by perfusion with Sorenson's phosphate buffer (pH 7.2) with 2% EM-grade paraformaldehyde and 1% EM-grade glutaraldehyde. Eyes were then harvested as follows, a slit was made in the cornea to aid in diffusion, and the tissue was placed in 3% glutaraldehyde in Sorenson's phosphate buffer overnight. Tissue was washed with 0.2 M cacodylate buffer in 5% sucrose, post-fixed in 1% OsO_4, embedded, sectioned, and viewed by transmission EM (TEM).

The spheres were embedded in 2% low temperature agarose. They were post fixed in 2% osmium tetroxide in 0.1 M sodium cacodylate buffer with 3% potassium ferrocyanide, enblock stained with 2% aqueous uranyl acetate, dehydrated through a series of alcohol washes, followed by propylene oxide. They were infiltrated and embedded in epon araldite and polymerized in a 70°C oven overnight.

For EM imaging of alkaline phosphatase, we developed a modification of the protocol described by Contini and Raviola (4). Animals were perfusion-fixed, as described above, and the eyes were harvested. Retinae were then removed, embedded in 4% LMP agarose/1× PBS and 100-mm vibratome sections prepared. The sections were then placed in 3% glutaraldehyde for 30 min, rinsed in PBS buffer, heated in PBS at 65°C for 30 min, and thoroughly rinsed with 5% sucrose in 0.2 M cacodylate buffer to eliminate phosphate ions. Sections were then incubated overnight with mild shaking in a beta-glycerophosphate, alkaline lead citrate solution (5). Samples were thoroughly rinsed in cacodylate buffer and postfixed in 3% glutaraldehyde. Selected samples were stained with osmium-ferrocyanide and uranly acetate; others were left unstained to better appreciate the alkaline phosphatase staining.

Neural Stem Cell Cultures From Adult SVZ. Neurobasal medium containing 1% Pen-Strep, 2 mM L-glutamine, 1× N2 supplement, 1× B27 supplement, 20 ng/mL hrEGF, 20 ng/mL human bFGF, 50 μg/mL BSA, and 20 μg/mL heparin. Adult C57BL/6 male mice were used for SVZ cultures. The brain was removed in ice-cold PBS plus 1 mg/mL glucose, and the hindbrain and midbrain were removed including the cerebellum. SVZ was separated from the anterior portion of the rostral migratory stream, minced, and placed in an enzyme mixture (Trypsin 0.25 mg/mL, DNaseI 0.05%, 0.2 mg/mL EDTA, and 10 mM Hepes, pH 7.4). The tissue was incubated for 7 min at 37°C, triturated 10 times, and repeated for a second round. The digestion was stopped by adding 2× tryspin inhibitor (2 mg/mL ovomucoid) and passed through a cell strainer (40 μm; BD BioSciences Catalog # 352340). The cells were pelleted and resuspended in growth medium. Spheres usually appeared within 3–5 days, and samples were passaged after 10 days in culture. On day 5, half of the medium was replaced with fresh medium.

Retinal Stem Cell Cultures. Isolation and growth of CE-derived spheres were done as in Tropepe et al. (6), with minor modifications. Briefly, CE were isolated from 6- to 8-week-old C57BL/6 male mice by first puncturing the eye with a 16 ga needle. Sclera and cornea were removed with forceps under a dissecting microscope. Retina, along with CE and lens were isolated. After removal of the lens, CE were dissected free of the retina using fine gauge forceps. CE were placed in an enzyme mix (0.67 mg/mL hyaluronidase, 1.33 mg/mL trypsin, and 1.3 mg/mL kynurenic acid in HiLo ACSF) for 30 min with mechanical dissociation every 15 min. Trypsin inhibitor (2 mg/mL ovomucoid) was added to the cell suspension. Single cell suspensions were then centrifuged for 5 min at 1,000 rpm, and supernatant was removed. Cells were resuspended in Neurobasal medium containing B27 supplement, penicillian/streptomycin, 2 mM l-glutamine, and supplemented with growth factors. Growth factor concentrations were Fgf-2 at 20 ng/mL, EGF at 20 ng/mL, and heparin at 2 μg/mL. Growth factors were replenished after 3 days. Cells were grown for 7 days before differentiation or passage.

Initially, we performed a series of side by side experiments (6, 7) using the culture medium described above and the medium used by Tropepe and colleagues (DMEM/F12, 6% glucose, −0.5% $NaHCO_2$, 0.05 M Hepes, 2 mM l-glutamine, 100 μg/mL transferrin, 60 μM putrescine, 30 nM selenium, 20 nM progesterone, 25 μg/mL insulin, 10 ng/mL Fgf-2, 20 ng/mL EGF, and 2 μg/mL heparin) (5, 6). The efficiency in sphere production was similar or slightly better using the medium described above. More importantly, gene expression analysis using RT-PCR was indistinguishable using spheres grown in the 2 different types of medium and histological analysis provided the same results. TEM analysis of human and mouse spheres from the van der Kooy lab grown in their medium were indistinguishable from spheres prepared in our lab using the aforementioned protocol.

CE-differentiation was carried out according to described methods (6, 7). Briefly, 7-day-old spheres were transferred to 24-well dishes with poly-l-ornithine laminin-(Sigma and Invitrogen provided indistinguishable results) coated round coverglass in neurobasal medium containing B27 supplement, penicillin/

streptomycin, 2 mM l-glutamine, and supplemented with 1% FBS.

P0 Retinal Sphere Cultures. P0 retinal cultures were carried out as described in ref. 8. Briefly, retinae were dissected in ice-cold 1× HBSS with 3% D-glucose and 0.1 M HEPES pH 7.4. Samples were then placed in a 0.25% trypsin solution in HBSS and incubated for 5–20 min at 30°C until the retinae were dissociated. To inactivate the trypsin, we added FBS to a final concentration of 20%, and the cells were pelleted by spinning at 1,500 rpm and resuspended in medium. The medium was DMEM/F12 with penicillin/streptomycin, 1× N2 supplement, and 1% FBS. Cultures were plated at 250,000 cells per mL. Fresh medium was added after 5 days, and cultures were analyzed after 7 days.

Computational Analysis of Dual Beam FIB Dataset. Artifacts of FEI's DualBeam collection method were removed from outside of the region of interest of serial section TIF images using Adobe Photoshop CS3 (Adobe Systems Inc.). This 3D region of interest containing an entire neurosphere was then fully aligned in translation and rotation using AutoAligner. (Bitplane Inc.). The following procedure was undertaken using Imaris (Bitlane, Inc.). Within that 3D volume, melanosomes were segmented by their intensity and size characteristics. The centroid of intensity of each melanosome was determined. Subsequently, we used this set of extracted 3D Cartesian coordinates for further analysis in Matlab (The Mathworks).

A program was written in Matlab that performed the following analysis (code is available upon request):

(A) The 3D rectangular region of interest containing an entire neurosphere was subdivided into a 3D grid with gridlines equally spaced in X– Z with a defined distance equal to 3.5 μm to represent the smallest possible nucleus in the eye (rod photoreceptor). In this way, we can be sure to avoid missing any nuclei in the CE-derived spheres. Among 383 cells in CE-derived spheres analyzed by morphometric analysis, none of them were smaller or equal to this dimension.

(B) Using the set of 3D Cartesian coordinates of the melanosome centroids, each subdivided region of interest (ROI) was queried for the presence or absence of a melanosome within its bounds.

(C) The centroids of each subdivided ROI that did not contain any pigmented melanosomes (negative ROI) were outputted as a set of spheres with a diameter of 3.5 μm into the original Imaris dataset containing the demarcated melanosome centroids for reanalysis.

This set of negative ROI's in the original CE-derived sphere were then examined on serial sections manually to determine whether there was a nonpigmented cell in this region of the sphere. Such a cell could be a potential retinal stem or progenitor cell. Each individual negative ROI was looked at in the context of the 3D boundary of the cell(s) that contained it and the nearest melanosome centroids. Upon detailed 3D inspection, if this cell(s) was found to actually contain a melanosome, then the negative ROI was determined to be a false negative. This procedure was repeated with the entire set of negative ROIs.

Affymetrix Gene Expression Analysis. All arrays passed quality metrics provided by Affymetrix GCOS software. The variability within samples of each type was modest when compared with the differences between groups, see principal components analysis (PCA) plot. Three arrays were analyzed for each sample (primary CE, CE spheres, adult retina). The genes that were present in the adult retina and CE and were downregualted in the CE spheres were eliminated because these were primarily retinal genes that were the result of inevitable cross contamination of the primary CE samples with retinal RNA. A total of 19,776 probe sets passed this filter and were present at least once in CE or CE spheres. Of these 19,776 probe sets, 15,066 were unchanged or modestly changed with <2-fold difference when comparing primary CE to CE spheres or were not statistically significant on more than a 2-fold basis on a false discovery rate of 5%. Of the 4,700 probe sets that were reliably different in the CE-spheres compared with the primary CE by at least 2-fold with a false discovery rate of 5% based on a *t* test, 4,055 were up-regulated in the primary CE as compared with the CE spheres and 645 were down-regulated in the primary CE as compared with the CE spheres.

1. Donovan SL, Schweers B, Martins R, Johnson D, Dyer MA (2006) Compensation by tumor suppressor genes during retinal development in mice and humans. *BMC Biol* 4:14.
2. Dyer MA, Cepko CL (2000) p57(Kip2) regulates progenitor cell proliferation and amacrine interneuron development in the mouse retina. *Development* 127:3593–3605.
3. Johnson DA, Donovan SL, Dyer MA (2006) Mosaic deletion of Rb arrests rod differentiation and stimulates ectopic synaptogenesis in the mouse retina. *J Comp Neurol* 498:112–128.
4. Contini M, Raviola E (2003) GABAergic synapses made by a retinal dopaminergic neuron. *Proc Natl Acad Sci USA* 100:1358–1363.
5. Gustincich S, Feigenspan A, Wu DK, Coopman LJ, Raviola E (1997) Control of dopamine release in the retina: a transgenic approach to neural networks. *Neuron* 18:723–736.
6. Tropepe V, et al. (2000) Retinal stem cells in the adult mammalian eye. *Science* 287:2032–2036.
7. Coles BL, et al. (2004) Facile isolation and the characterization of human retinal stem cells. *Proc Natl Acad Sci USA* 101:15772–15777.
8. Reh TA, Fischer AJ (2006) Retinal stem cells. *Methods Enzymol* 419:52–73.

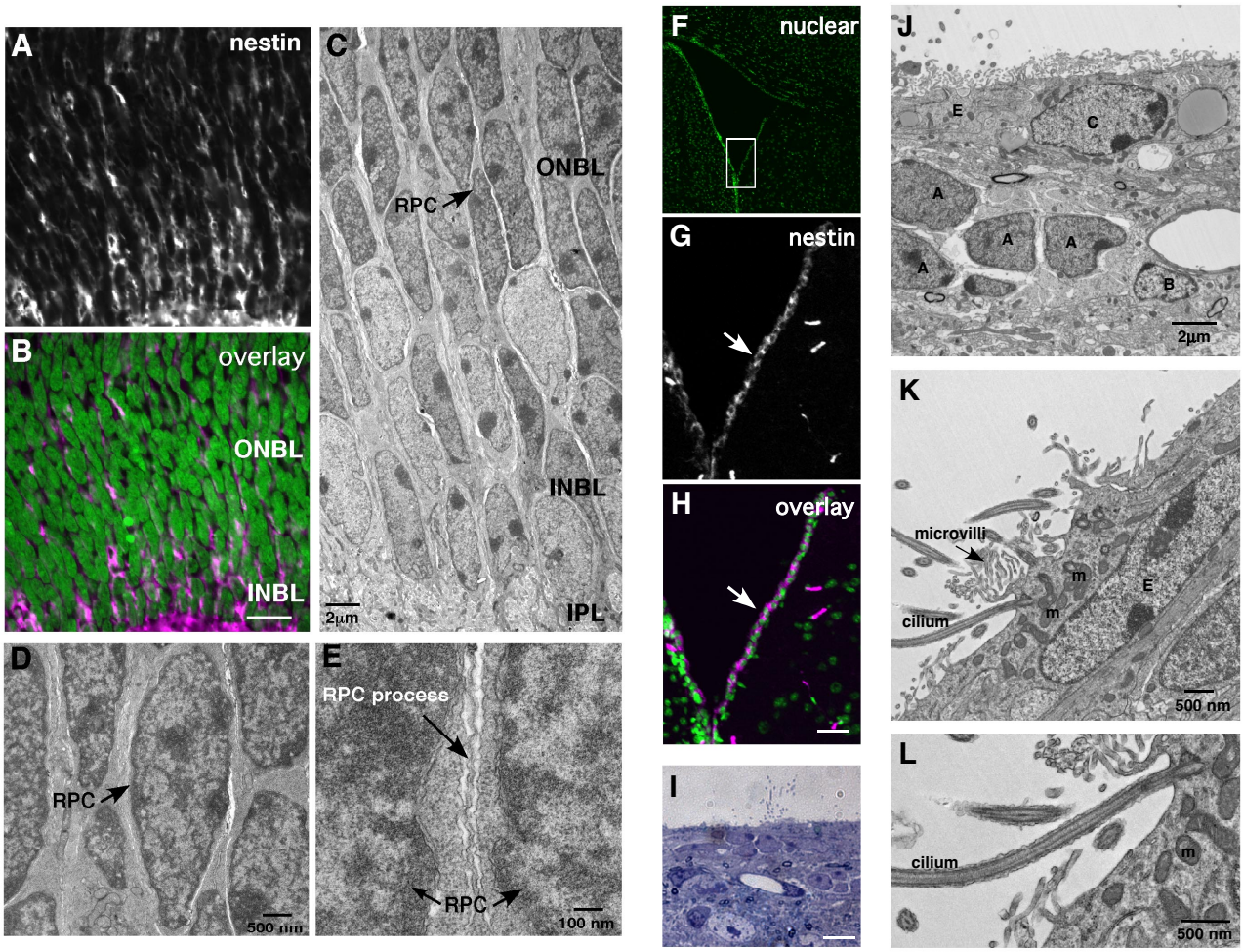

Fig. S1. Retinal progenitor cells and neural stem cells do not contain pigment, membrane interdigitations, or epithelial junctions. (*A* and *B*) Nestin immunofluorescense in a P0 mouse retina. At this stage of development, there are abundant retinal progenitor cells in the center of the retina, and these cells express nestin. The nuclei are stained fluorescent green with Sytox Green. (*C–E*) TEM analysis of retinal progenitor cells in the P0 retina. At this stage, the retinal progenitor cell nuclei and cell bodies are primarily localized to the outer neuroblastic layer (ONBL). The cells are typically in an elongated shape (*D*) along the apical-basal axis and extend a single small process to the apical and basal surfaces (*E*) to facilitate their interkinetic nuclear migration through the cell cycle. Abbreviations: RPC, retinal progenitor cell; ONBL, outer neuroblastic layer; INBL, inner neuroblastic layer; IPL, inner plexiform layer. (Scale bars in *A and B*, 10 μm.) (*F–H*) Nestin immunofluorescense in the adult SVZ where neural stem cells reside. The nuclei are stained fluorescent green with Sytox Green. (*I*) Toluidine blue stained histological section of the adult mouse SVZ showing the unique morphological features of this region of the brain. (*J–L*) TEM analysis of SVZ cells in the adult mouse brain. The distinct cell types can be readily identified in these images including the ependymal cells (*E*) and the A,B and C cell types. (*J* and *K*) The ependymal cells are characterized by their extensive microvilli and cilium and abundant mitochondria (m). Abbreviations: m, mitochondria. (Scale bars in *C*, 25 μm; *D*, 10 μm.)

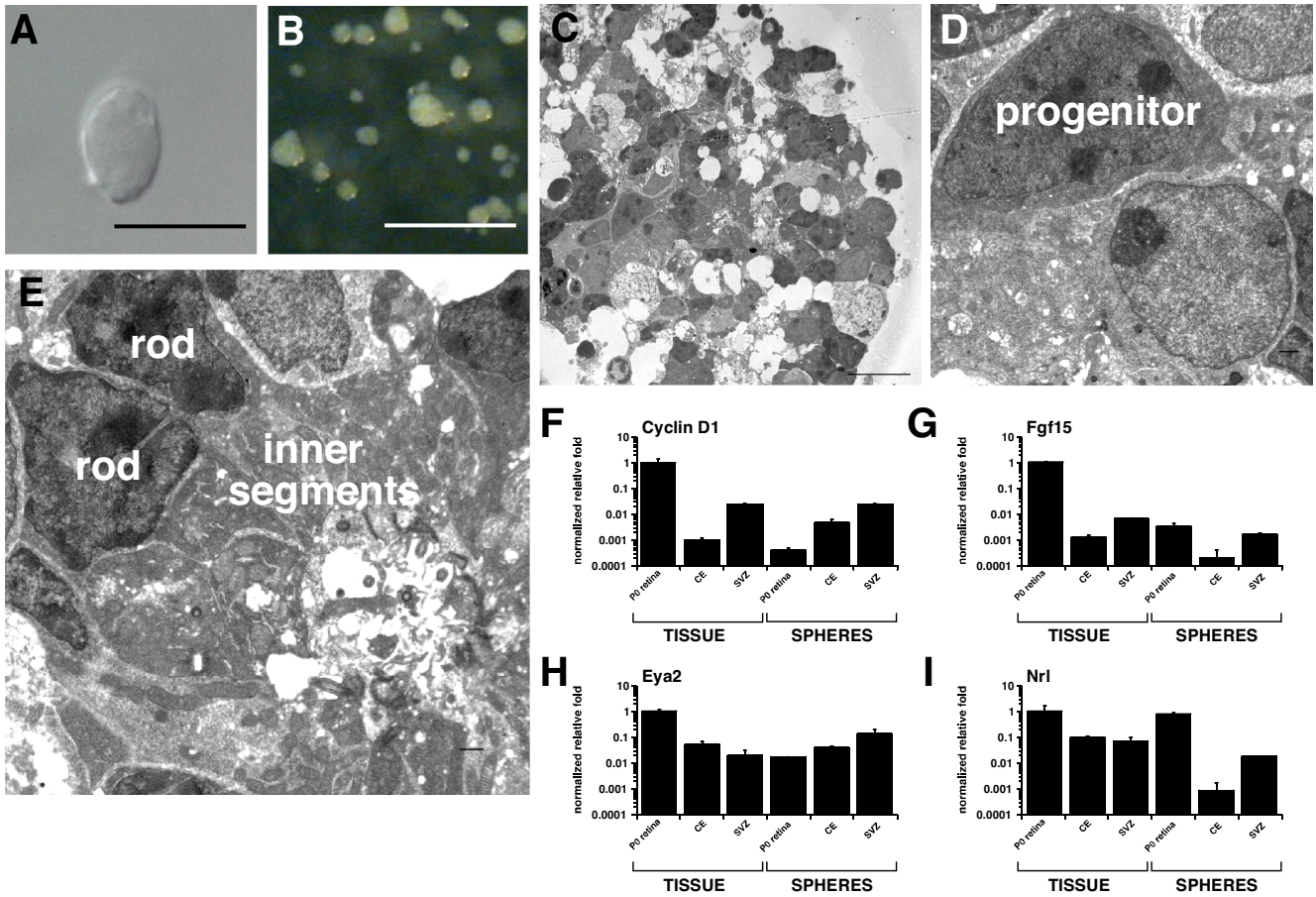

Fig. S2. Retinal progenitor cell derived spheres contain differentiated neurons. According to the retinal stem cell model, CE-derived spheres should be made up primarily of retinal progenitor cells. To provide a benchmark for comparison, we grew spheres from P0 mouse retinal progenitor cells. (*A*) Retinae were dissociated into a single-cell suspension that contained retinal progenitor cells. (*B*) When plated in stem cell medium these cells could form spheres after 7–10 days in culture. (*C–E*) TEM analysis revealed that the majority of the cells in the retinal progenitor cell derived sphere were differentiated retinal neurons such as photoreceptors and a small subset of cells with morphological features of retinal progenitor cells. This finding suggests that when retinal progenitor cells are cultured under conditions that are similar to those used for CE-derived spheres they differentiate rather than maintaining their progenitor status. These data were inconsistent with the model proposing that CE-derived spheres were made up of retinal progenitor cells. We selected P0 retinae for these studies because P0 retinal progenitor cells are competent to produce rods, bipolar cells, and Müller glia. These were the same cell types produced from CE-derived spheres making them equivalent. (*F–I*) Real time RT-PCR confirmed that the retinal progenitor derived spheres were depleted of retinal progenitor cells expressing cyclin D1, Fgf15, and Eya2. There was an increase in differentiation markers such as Nrl. (Scale bars in *A and C*, 10 μm; *B*, 1 mm; *D and E*, 1 μm.)

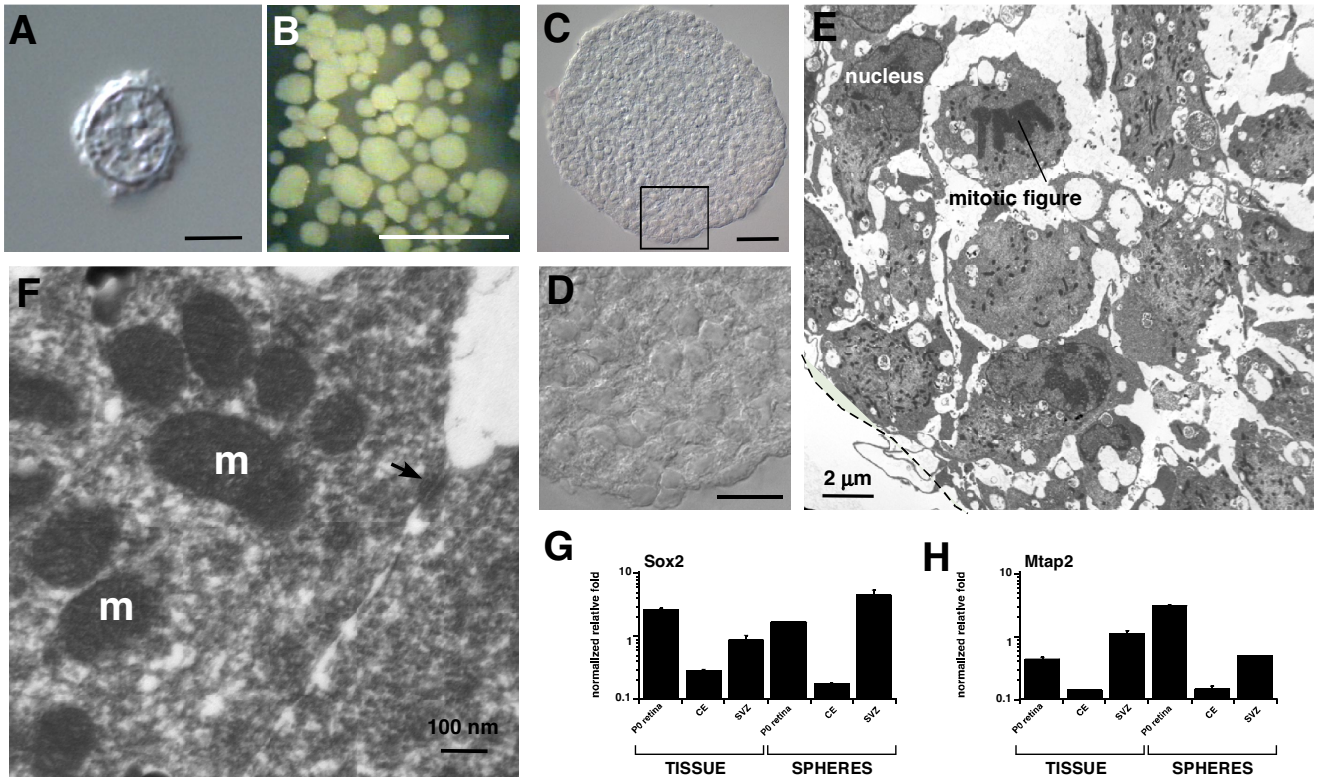

Fig. S3. Characterization of SVZ-derived neurospheres. We have shown that the cells in the CE-derived spheres do not resemble retinal progenitor cells. To compare the CE-derived cells to neural stem cells we generated SVZ-derived neurospheres. (*A*) The SVZ was isolated from adult C57BL/6 male mice, dissociated, and plated in stem cell medium at clonally density. (*B*) After 7–10 days, these cells grew into clonogenic spheres typical of neural stem cells. (*C* and *D*) These neurospheres were made up of undifferentiated cells that were not pigmented as shown in these DIC images of SVZ-derived sphere cryosections. (*E* and *F*) TEM analysis revealed that the spheres were made up of undifferentiated cells that lack pigment and membrane interdigitations, and epithelial junctions found in the CE or CE-derived spheres. Occasionally, gap junctions were identified (arrow). (*G* and *H*) Genes associated with stem cells, such as Sox2, were increased in SVZ-derived neurospheres, and genes associated with neuronal differentiation (Mtap2) were decreased in the spheres. Abbreviations: m, mitochondria. (Scale bars in *A*, 2 μm; *B*, 1 mm; *C*, 25 μm; *D*, 10 μm.)

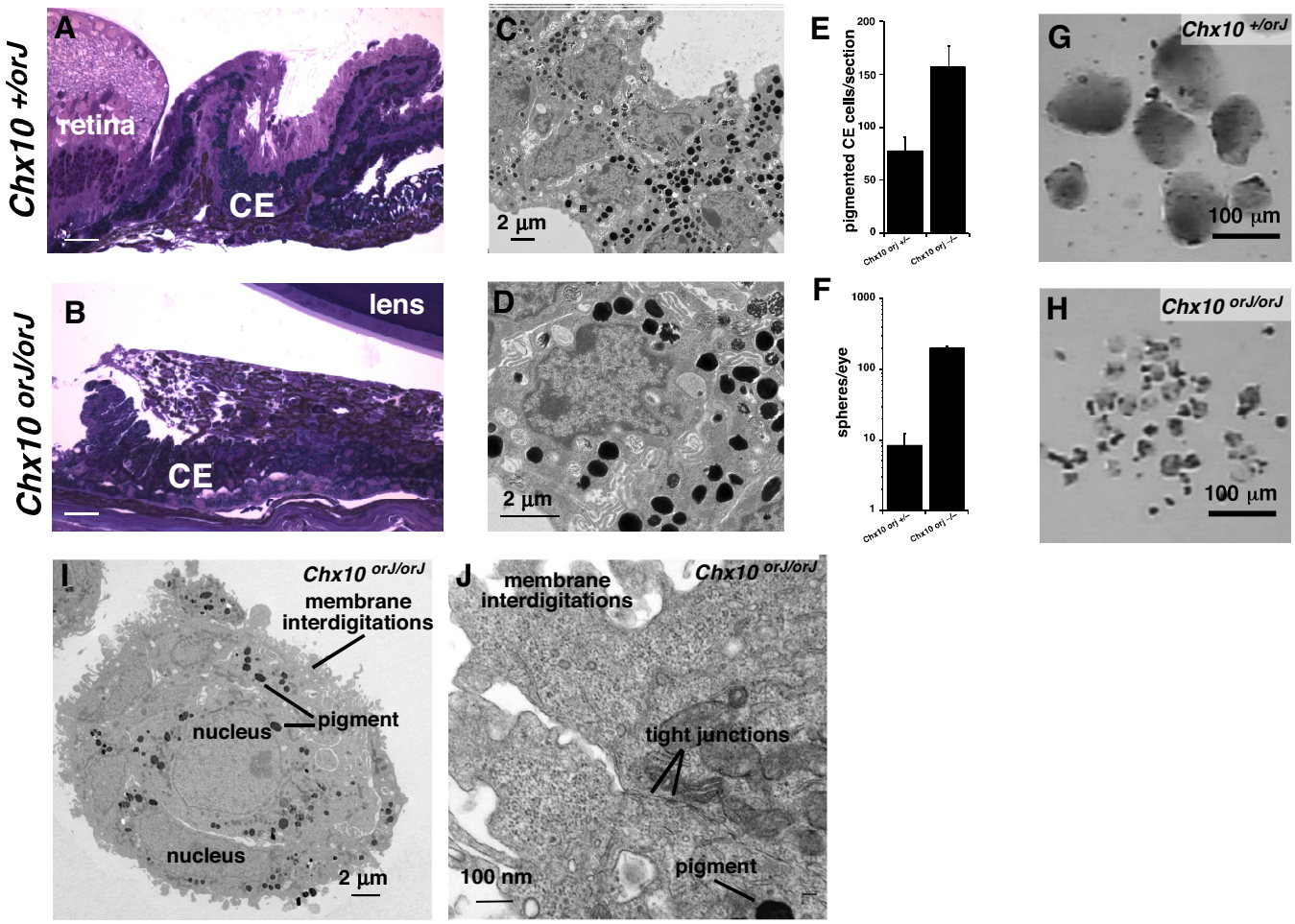

Fig. S4. The Chx10orJ/orJ eye has increased pigmented CE cells. It has been reported that there is an increase in sphere production from the CE of *Chx10orJ/orJ* mouse eye. If the cell of origin for the CE-derived spheres is a pigmented CE cell then we would predict that there would be an increase in pigmented CE cells in these eyes. (*A* and *B*) Comparison of toluidine blue stained sections from adult *Chx10orJ/+* and *Chx10orJ/orJ* mice showed a marked increase in pigmented CE cells. Very few, if any, nonpigmented CE cells were detected in these eyes. (*C* and *D*) Transmission electron microscopic (TEM) analysis of CE from *Chx10orJ/orJ* mice confirmed the increase in pigmented CE cells. (*E* and *F*) We scored the number of pigmented CE cells per section in transmission electron micrographs, and these data confirmed the observation that the *Chx10orJ/orJ* mice had an increase in the pigmented CE cells. This led to an increase in the efficiency of sphere production. (*G* and *H)* Despite the increase in the efficiency of sphere production, the spheres were smaller from the *Chx10orJ/orJ* mice. (*I* and *J*) TEM analysis of CE-derived spheres from *Chx10orJ/orJ* mice showed that all of the cells had the features of pigmented CE cells including pigment, membrane interdigitations, and epithelial junctions. Abbreviations: CE, ciliary epithelium. (Scale bars in *A* and *B*, 10 μm.)

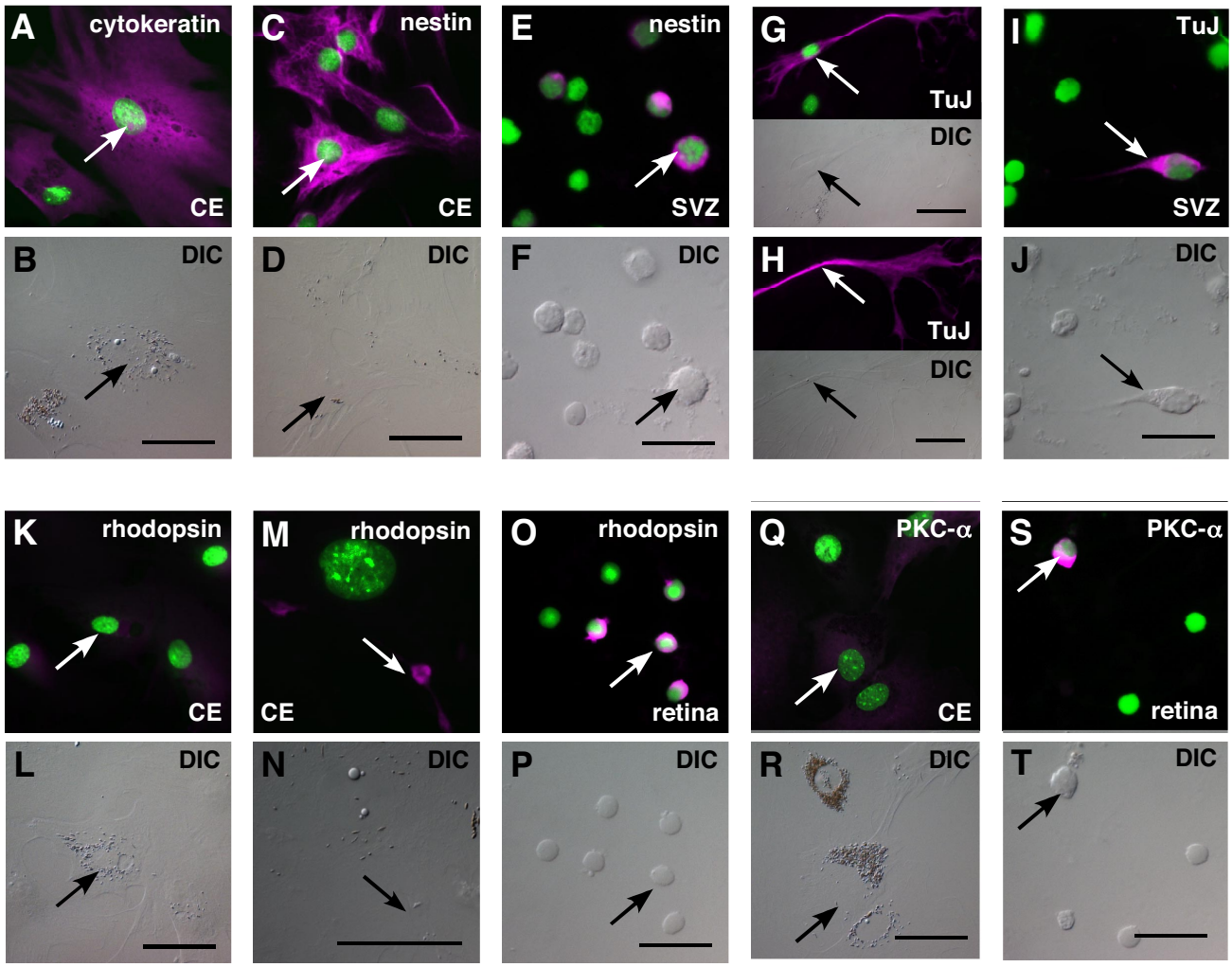

Fig. 55. Differentiation cultures from mouse CE spheres resemble pigmented CE cells. CE spheres were cultured for 21 days under differentiation conditions to induce neuronal transdifferentiation. (*A* and *B*) Cytokeratin is a protein expressed in the CE but not the retina. Virtually all of cells in the differentiation cultures were flat, pigmented cells that expressed cytokeratin (purple). The nuclei are shown in green using Sytox Green and the pigment is visualized using DIC imaging of the same field. (*C* and *D*) Nestin is a neural progenitor/stem cell protein, and this was expressed in a subset of cells with pigmented epithelial morphology. As a positive control, we used dissociated cells from the SVZ of an adult mouse brain (*E* and *F*). TuJ is a neuronal marker, and it was expressed in a subset of flat, pigmented, epithelial cells. However, in some cases, as shown here (*G* and *H*), the edge of the epithelial cell curled up to produce this pattern of immunofluorescense that vaguely resembles a neuron. This cell contains pigment granules throughout this cell body (arrow in *H*). (*I* and *J*) As a positive control, we used dissociated cells from the SVZ of an adult mouse brain. (*K* and *L*) Rhodopsin is a protein found in rod photoreceptors and it was not expressed in any of the cells from the CE differentiation culture. (*M* and *N*) Occasionally, the flat, pigmented, epithelial cells curled up to trap the antibody resulting in nonspecific immunofluorescense, resembling a rod photoreceptor. It is important to note that this immunopositive structure does not contain a nucleus and may explain the false positive cells detected in previous studies. (*O* and *P*) As a positive control for rhodopsin immunostaining, we used dissociated adult retinae. (*Q* and *R*) PKC-α (a bipolar marker) was not expressed in any of the cells from the CE differentiation culture. (*S* and *T*) As a positive control for PKC-α immunostaining, we used dissociated adult retinae. Abbreviations: CE, ciliary epithelium; DIC, differential interference contrast microscopy; SVZ, subventricular zone. (Scale bars, 10 μm.)

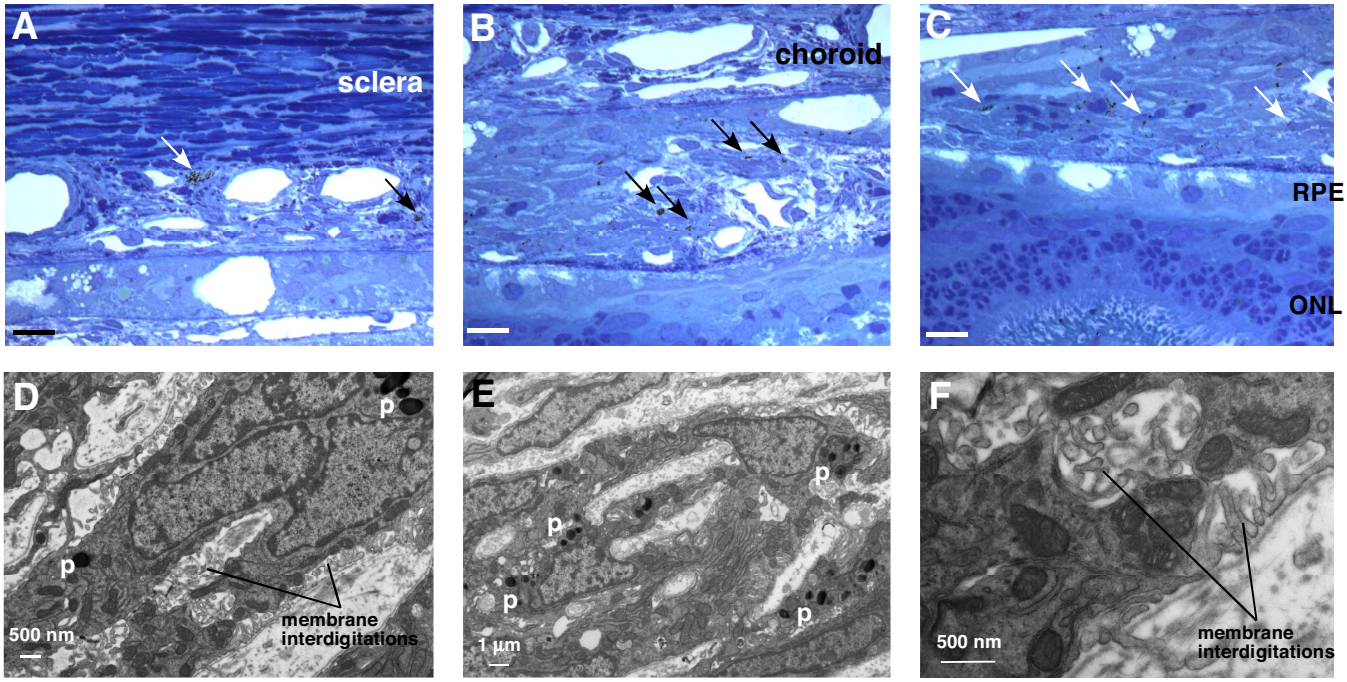

Fig. S6. Characterization of CE-derived sphere injections into newborn rat eyes. (*A–C*) Three examples of 1-μm thick sections of rat eyes 21 days after CE-derived spheres were injected into the subretinal space at P0. There were abundant pigmented cells (arrows) in this albino rodent eye indicating that the CE sphere-derived cells maintained their pigmentation. (*D–F*) To characterize the other features unique to the pigmented CE, these specimens were then sectioned at 50 nm for TEM analysis. Two examples of clusters of pigmented cells with morphological features of CE cells are shown (*D* and *E*), and a high magnification view of the membrane interdigitations characteristic of these cells. Abbreviations: ONL, outer nuclear layer; p, pigment. (Scale bars in *A–C*, 10 μm.)

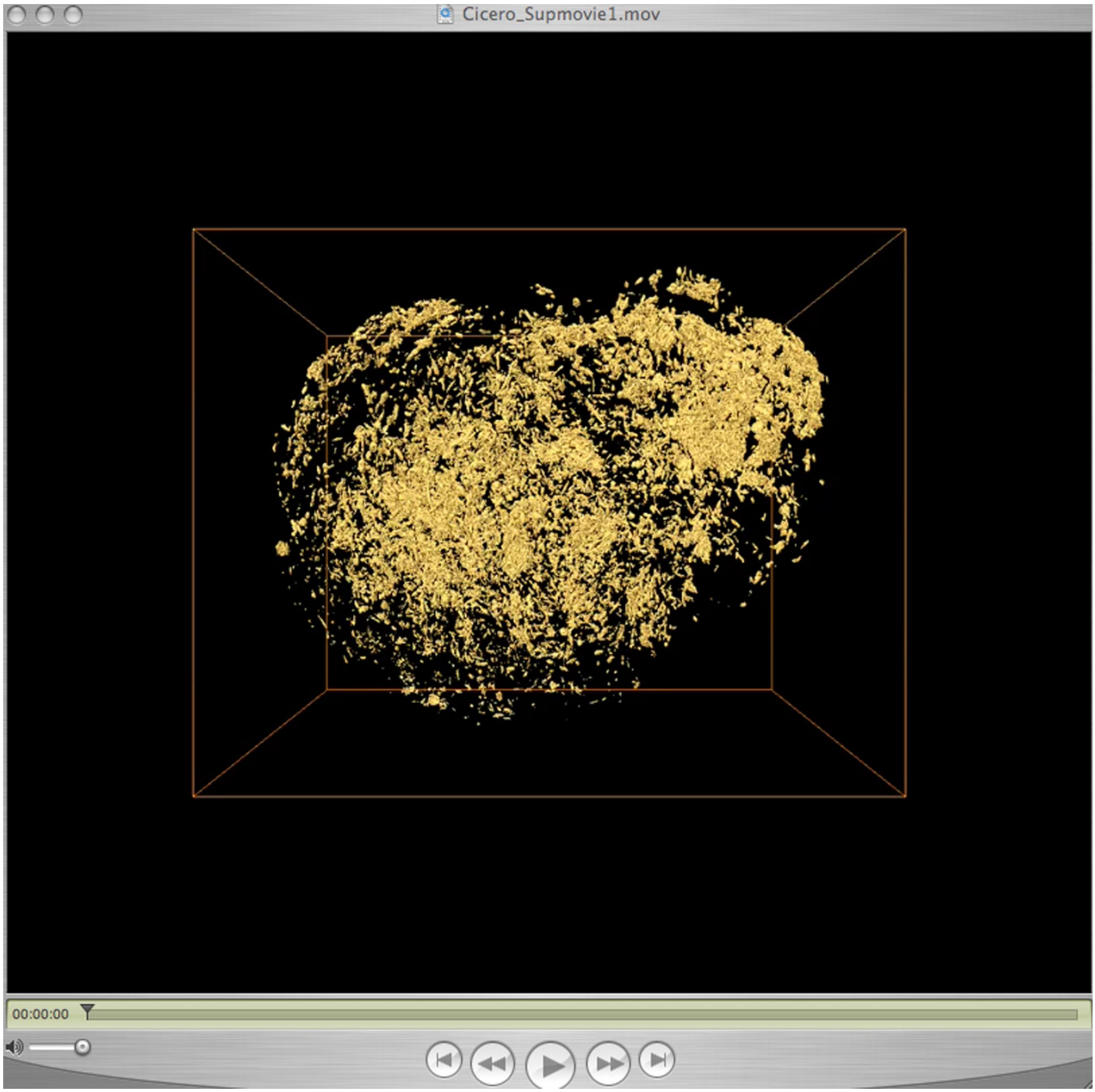

Movie S1. 3D reconstruction of TEM images of CE sphere. A representative sphere was analyzed by dual beam FIB using 100-nm sections to capture TEM images of every cell in the sphere. Each section was imaged, aligned, and analyzed for the presence of retinal stem cells lacking pigment. Spheres are ≈100 μm in diameter. Therefore, it takes 900–1,000 individual sections and images to visualize an entire sphere with TEM resolution. This is a rotational movie of the 3D reconstructed sphere with the image intensities reversed. White areas represent the pigmented portion of the sphere, and black areas represent the cytoplasm and other cellular structures. The movie will play on Quicktime player and should be transferred to the hard drive of the computer to ensure uninterrupted projections.

Movie S1

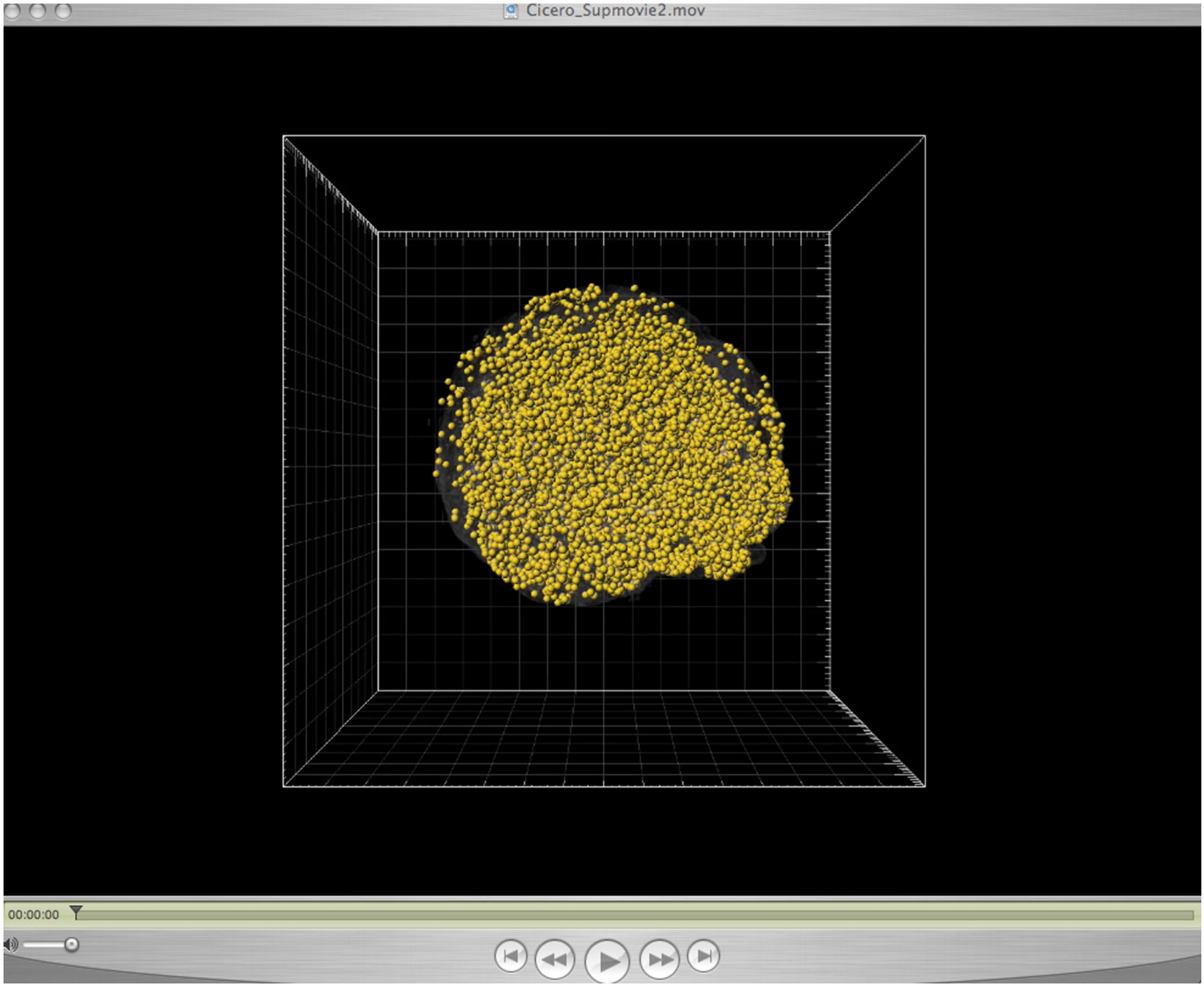

Movie S2. Pigment granules in CE-spheres using dual beam FIB. The dataset shown in Movie S1 was analyzed using Imaris software to identify and mark the coordinates of every pigment granule in the sphere. These are represented with gold spheres. This identification of each pigment granule allowed us to determine the distance between pigment granules and then analyze the serial TEM images at those coordinates to determine whether there was a nonpigmented retinal stem cell present. This is a rotational movie of the 3D reconstructed sphere with the image intensities reversed. Pigment is represented by gold spheres of the same diameter as the pigment granules. The movie will play on Quicktime player and should be transferred to the hard drive of the computer to ensure uninterrupted projections.

Movie S2

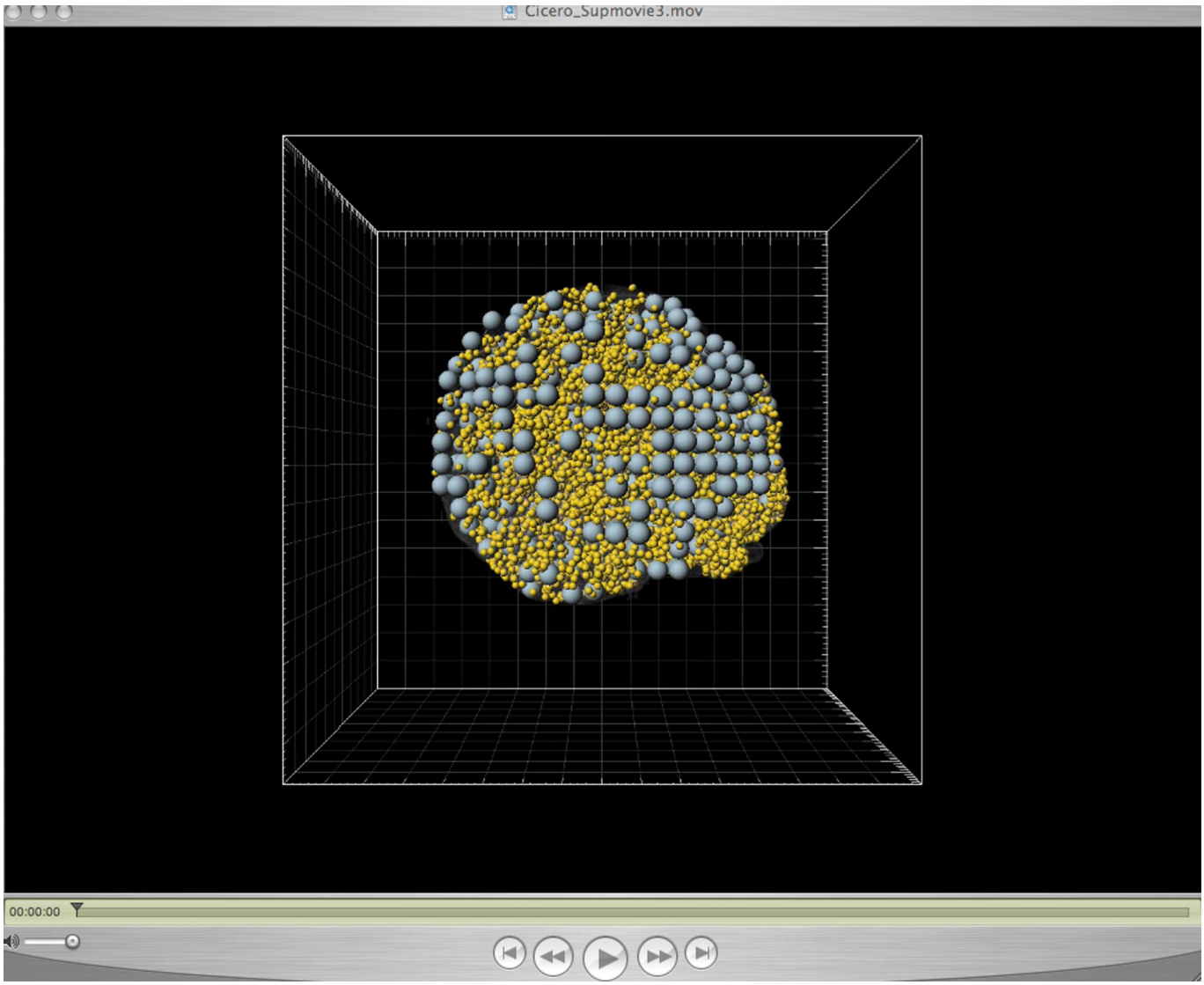

Movie S3. Pigment-free regions of the CE-derived sphere. As in Movie S2, the pigment is shown in gold. The region between pigment granules was then analyzed to determine whether a nonpigmented cell could fit in that space. These spaces are shown as white spheres. Four hundred ninety-four individual regions were identified that lacked pigment and were sufficiently large to contain a nonpigmented retinal or neural stem cell. Each of these regions was then individually analyzed in the original serial TEM images to determine whether there were any nonpigmented cells in those regions. None of the 494 regions contained any nonpigmented cells. This demonstrates that the entire CE-derived sphere is made up of pigmented CE cells. This is a rotational movie of the 3D reconstructed sphere with the image intensities reversed. The movie will play on Quicktime player and should be transferred to the hard drive of the computer to ensure uninterrupted projections.

Movie S3

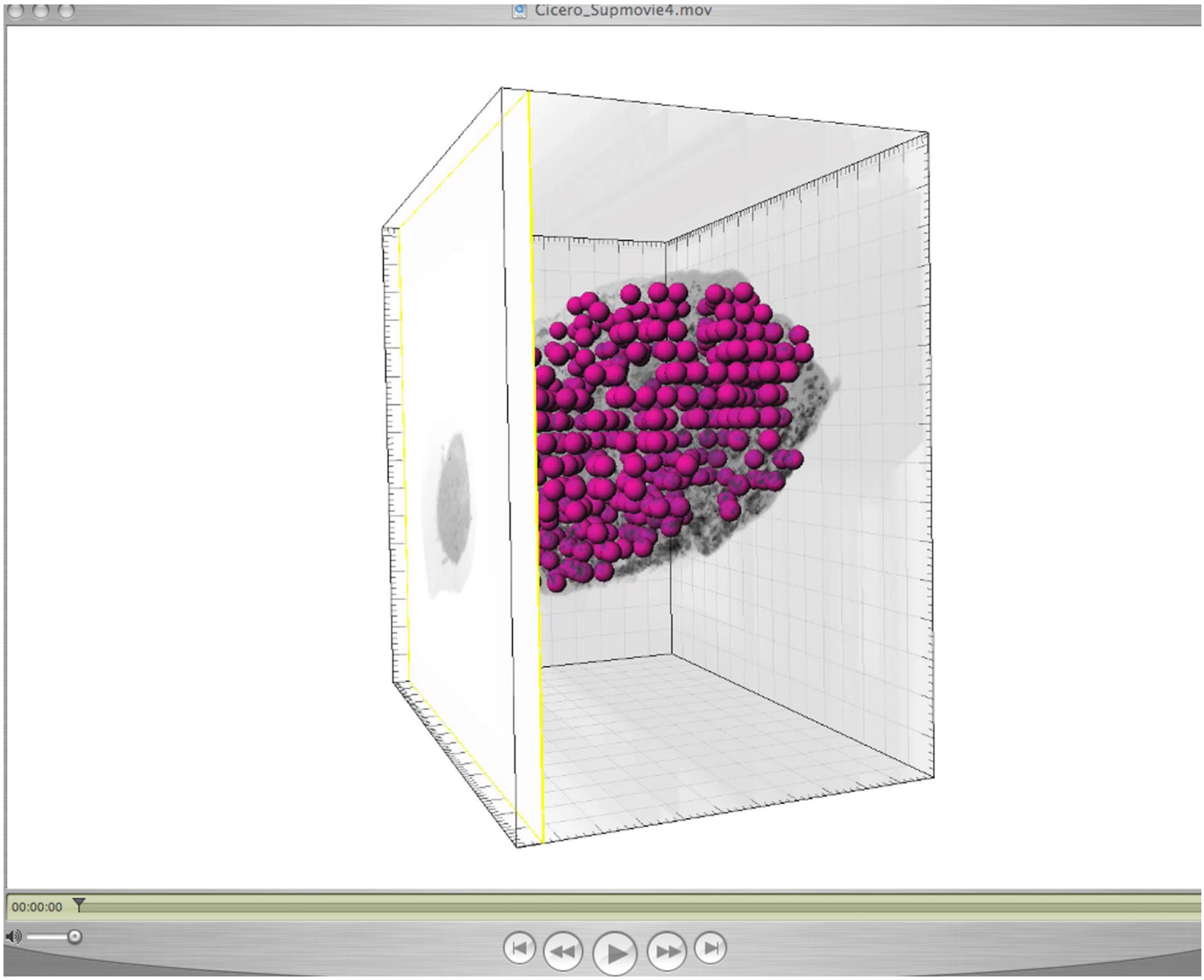

Movie S4. Serial sections of 3D reconstruction of CE sphere. In this view, the entire sphere is shown with the pigment as black, and the cell bodies and other structures lighter shades. The shading of the images are reversed from that shown in Movie S1–S3. The purple spheres represent the volumes lacking pigment that are large enough to fit a retinal stem/progenitor cell. In this movie, the individual sections are projected in 3D with the volumes lacking pigment shown. The movie will play on Quicktime player and should be transferred to the hard drive of the computer to ensure uninterrupted projections.

Movie S4

Table S1. Morphometric analysis of CE-derived spheres

Sample*	Process length, μm, mean ± SD†	Density, process/μm^2, mean ± SD‡	Cell body area, μm^2, mean ± SD	Nuclear area, μm^2, mean ± SD	Nuc/cyto ratio	Nuclear volume, μm^3, mean ± SD §	Pigment
CE	0.76 ± 0.15	2.78 ± 0.42	66.84 ± 4.60	13.01 ± 0.89	0.19	40.41 ± 3.82	yes
CE spheres	0.42 ± 0.15	1.24 ± 0.16	34.43 ± 3.57	13.33 ± 1.32	0.39	44.72 ± 6.65	yes
SVZ spheres	0.99 ± 0.63	0.097 ± 0.075	42.46 ± 2.82	18.53 ± 1.24	0.44	69.10 ± 6.91	no

*90 cells for each category were scored.

†Processes were measured from cell body until they were no longer visible. Because the basal and lateral interdigitations fold torturously these measurements are underestimations of total length. This was also the case with some of the CE sphere process, whereas the SVZ cell processes were more likely to be found in entirety.

‡All processes with uniform diameter were counted only if the junction of cell body and process was visible.

§Equivalent oblate volume.

Table S2. Affymetrix gene expression microarray comparison of CE and CE-derived spheres

Gene*	Unigene	Cesphere†	Primary CE†	Log ratio‡	Fold§	*P* value	Function
Cdkn2b	Mm.423094	8.89	4.90	5.76	54.03	3.38E-07	cell cycle, G1/S inhibitor
Bub1	Mm.2185	6.39	3.08	4.77	27.33	3.74E-06	cell cycle, M-phase, promotes division
Cdkn1a	Mm.195663	7.82	4.72	4.46	22.08	5.61E-05	cell cycle, G1/S inhibitor
Cxcl1	Mm.21013	6.98	4.07	4.20	18.39	1.28E-06	cell cycle, promotes cell division
Ereg	Mm.4791	7.01	4.12	4.17	17.97	5.85E-04	growth factor, promotes proliferation
Igfbp3	Mm.29254	9.32	6.44	4.16	17.93	2.21E-05	regulates cell growth
Ccnb1	Mm.260114	6.85	4.04	4.06	16.73	1.42E-04	cell cycle, promotes proliferation
Nek2	Mm.33773	6.26	3.55	3.90	14.97	6.41E-04	cell cycle, M-phase
Cdca8	Mm.28038	6.84	4.22	3.78	13.73	3.01E-05	cell cycle, proliferation
Prc1	Mm.227274	6.89	4.28	3.77	13.64	2.42E-04	cell cycle, cytokinesis
Gdnf	Mm.4679	5.75	3.18	3.71	13.10	7.64E-07	growth factor, promotes cell division
Cdca5	Mm.23526	6.54	4.01	3.65	12.57	9.06E-07	cell cycle, cytokinesis
Mki67	Mm.4078	7.45	4.94	3.62	12.27	6.94E-05	marker of proliferating cells
Cenpf	Mm.129746	6.77	4.31	3.56	11.77	4.56E-04	centromere, proliferation
Bmp1	Mm.27757	9.14	6.72	3.48	11.18	8.99E-06	growth factor
Cxcl5	Mm.4660	6.61	4.23	3.44	10.82	2.19E-05	cell cycle, promotes cell division
Kif2c	Mm.247651	6.25	3.90	3.40	10.52	9.11E-06	centromeres, M-phase
Kif23	Mm.259374	6.58	4.25	3.36	10.30	2.62E-05	cytokinesis
Tgfb1	Mm.248380	6.91	4.64	3.27	9.66	6.90E-06	TGF-beta, promotes cell division
Myc	Mm.2444	6.58	4.41	3.13	8.75	2.38E-04	cell cycle, promotes cell division
Nuf2	Mm.151315	6.02	3.86	3.12	8.71	2.24E-03	cell cycle, M-phase
Cenpi	Mm.34903	5.40	3.25	3.09	8.54	9.90E-05	cell cycle, M-phase
Sgol1	Mm.153202	5.55	3.43	3.06	8.36	8.18E-04	chromatid adhesion, M-phase
Ndc80	Mm.225956	5.40	3.57	2.63	6.19	1.39E-04	cell cycle, M-phase
Ccnd1	Mm.273049	8.22	6.44	2.57	5.92	2.64E-05	cell cycle, G1/S cyclin D1
Cdca5	Mm.23526	5.64	3.92	2.48	5.57	1.43E-03	cytokinesis
Cgref1	Mm.45127	5.17	3.46	2.46	5.50	9.45E-04	cell cycle arrest
Cdca2	Mm.33831	5.21	3.54	2.41	5.31	4.87E-05	cell cycle, promotes cell division
Cdc6	Mm.20912	5.66	4.04	2.33	5.03	1.47E-04	cell cycle, DNA replication

*The majority of genes that were up-regulated in the CE-spheres compared with the primary CE were involved in cell cycle control/proliferation or secretory pathways. A representative list is shown for genes that are involved in cell cycle control/proliferation of all genes that were >5-fold increased with statistically significant *P* values.

†ln(MAS 5.0 signal + 20).

‡Log2ratio = log(exp(mean of ln(MAS5.0 + 20) group A)/exp(mean of ln(MAS5.0 + 20) group B))/log(2) (in other words the log base2 of the ratio of geometric means of stabilized MAS 5.0 signal.

§Fold Change = 2^abs(log2ratio) if log2ratio > 0; Fold Change = −1*2abs(log2ratio) if log2ratio < 0.

Table S3. Morphometric analysis of cells in S-phase in CE-derived spheres

Morphological feature	PCE, counts, %±SD[¶]	[^{3}H]-thy + CE-derived spheres, counts, %±SD**	SVZ-derived spheres, counts, %±SD[††]
pigment*	9/9;5/5;11/11	12/12; 9/9; 6/6	0/10;0/5;0/5
	100 ± 0%	100 ± 0%	0 ± 0%
membrane interdigitations[†]	9/9;5/5;11/11	12/12; 9/9; 6/6	0/10;0/5;0/5
	100 ± 0%	100 ± 0%	0 ± 0%
tight junctions[‡]	5/9;3/5;11/11	4/12; 7/9; 1/6	0/10;2/5;5/5
	38 ± 33%	42 ± 31%	46 ± 50%
adherens junctions[§]	8/9;5/5;11/11	8/12; 6/9; 3/6	8/10;4/5;0/5
	96 ± 6%	61 ± 9%	53 ± 46%

*A cell is scored as pigment + if it has at least one melanosome and a nucleus is visible.

[†]A cell is scored as having membrane interdigitations if it has at least one process that is uniform diameter and in contact with other processes.

[‡]A tight junction is defined as an area where the membranes come together and appear to fuse in TEM images with electron dense material at the junction where the membranes fuse.

[§]An adherens junction can be distinguished from a tight junction by the distance between the plasma membrane with the appearance of two distinct membranes. There is also a visible electron density on the intracellular side of each membrane.

[¶]PCE is the primary ciliary epithelium of an adult C57Bl/6 male mouse (≈6 weeks of age).

**A cell was scored as [^{3}H]-thy + if >10 silver grains were present. An average [^{3}H]-thy + cell had 37 ± 18 silver grains and an average [^{3}H]-thy– cell had 5 ± 4 silver grains per cell.

[††]Cells were isolated from the lateral wall of the lateral ventricle (including the SVZ) of adult C57Bl/6 male mice and cultured according to standard neural stem cell protocols.

Table S4. Antibodies used in the characterization of CE-derived spheres

Protein/dye	Company	Catalog no.	Vibratome/cryosection	Dissociated cell
GFAP	Sigma	G 3893	1:100	–
Recoverin	Chemicon	Ab5585	1:5000	–
PKC-α	Upstate	05–154	1:10000	–
Pax6	DSNB	Pax6	1:20	–
Rhodopsin	Dr. Molday		1:500	–
DAPI (5 mg:ml)	Sigma	D8417	–	1:2000
Sytox Green	Invitrogen	S7020	1:1000	–
Cytokeratin	Sigma	C2931	1:100	1:100
Nestin	Chemicon	MAB353	1:20000	1:20000
Chx10	ExAlpha	X1180P	1:500	–
b-III tubulin (Tuj1)	Covance	MMS-435P	1:500	1:1000
Map-2	Sigma	M1406	1:1000	1:2000

Table S5. QPCR probe and primer sequences

Gene	Forward	Reverse	Probe	Unigene
Sfrp2	GACCCGAGGGCATTTTCTCT	CGCCTGACATGGCAACCTA	TTTGGTCAGTCTGTTGGCTTATACC-GTGC	Mm.19155
Eya2	TGCACCCGTTACTCCCATTAC	CACCCGAAACCAGACCTACAG	CACGGGTCCCTGTGTTGTCGTTTCTC	Mm.282719
Fgf15	TGGCTAGACTTGATCATGAAC-CTAA	TCAGCAGCCTCCAAAGTCAGT	CCTGCCTGGCTGCCATCGGAG	Mm.3904
Lim1	GCTACGGGAACCATTTGTCTCA	GCGAGACCCCGCTACCA	CTCCTGAAATGAACGAGGCAGCCGT	Mm.4965
Recoverin	GCAGCTTCGATGCCAACAG	TCATGTGCAGAGCAATCACGTA	TACGCTGGACTTCAAGGA	Mm.439726
Chx10	TGAGGCAAGGCCCATGTC	CGGGAGTATGTCCAGGATGTCT	AGGCCCGCAATTACCCCCACG	Mm.4405
Pkca	CGCGAGGACAGCCTGTCT	AGAACCCTTCAAAATCAGATTGGT	CCACCAGATCAGCTGGTCATTGCTA-ACATA	Mm.222178
Gpi1	TCCGTGTCCCTTCTCACCAT	GGCAGTTCCAGACCAGCTTCT	CTCCCTGCCCAGAGCGCACC	Mm.589
Prox1	TTAGAACAGGCTCGTGGTGAGA	TGAAGCAAAGTAAATAGCAACTA-GTGACA	TGAGCTTGGCCGTGTGGACTTAGAGG	Mm.132579
Gapdh	CTCCACTCACGGCAAATTCA	CGCTCCTGGAAGATGGTGAT	AAGGCCGAGAATGGGAAGCTTGTCATC	Mm.333399
Rhodopsin	CATGCCAATATGCCCACCTT	GCACTGTGTTTCTGAACTCTTCAGA	AGGGAGCAGCTGAGTCCTTGATGCC	Mm2965
Btf3	TGGTGCAGACAGCCTGACTAGT	GTGCTTTTCCATCCACAGATTG	AGGAGACTGGCTGAAGCTCTGCCCAA	Mm371688
Calbindin	CACATGTAACTCTGTTTCGTGTA-TCCTT	TCACAATAAAGAATCCAGGCAATT-AA	AGTGTGTCCTCTGCTGGTTATTGGTGA-CAA	Mm277665
CRALBP	CTGTCCAGGGTGGAGGTCAT	CCCCAGCACCAAGGATCAC	TCCCTTCCTCTCCACCCATCTTGGA	
Crx	TCTGTGTGTTACAGACATGACC-ACTAA	CATCAAGCTTCTTTTGCATTTTGT	CTGAGCTGGGATGCTGTGGCTTGTATA-AA	Mm441911
Cyclin B1	CGGTGGGATTCAAGTGCATT	GCCAAGCAAGACATTAAACATCAT	TCTCAGTGCCCTCCACAGTGTTC	Mm260114
Cyclin D3	CTCTAGAACAATCCATGCTATA-TCTGAAG	TGAAGACGCCCCTCATGAC	TCCTGCCTATCCCCACAGTGTGCAC	Mm246520
Cyclin D1	CCCATGACCAGTGTGACTCAAA	TCAGACATGGCCCTAAACCTTCT	CAATGTGATCTCCCTTGATTCAAACGCA	Mm273049
Dct	CACCGTCGCTCATCTTGAGA	AATTGTCATTGCTAAGGCATCATC	AGGTGGAACTCTTCAGCGTGTGCTCT-TTAG	Mm19987
GFAP	ATCGAGAAGGTCCGCTTCCT	GGCTCGAAGCTGGTTCAGTT	AGCAAAACAAGGCGCTGGCAGC	Mm1239
Glut. Synthetase	GGTGCCAAGTTTGAGTGATGAG	ACTTTCCCGGTACTGCATCCT	CTTGGCTTAGAAGTGAGGCTCCCTTGA-GG	Mm210745
Gnat1	TGACCAATAATGAAGCCATGCT	TCTTTGCCCATGGTTGATCA	TGGCTCAGAGCAGAGTCCAACCCCTA	Mm284853
Hmga2	CCAGCTGTTTTCAGGGAGGTT	CAGTGAGCCATCTGCCAGTCT	TCAAAGGCCACGTGCCGCT	Mm157190
MitF	TTGTGAGCCAGACTTGTATATTC-TATTTT	AATCCCCTTGCTCAGAAAGCT	CCTCCTAAGTATTGTACCTTCAGCGTG-CAGTATCTGT	Mm333284
Msi2	CTGAGTGGCCCTTTGTTTAGGT	TCTGGTTGGGATGAGGAGTGA	TCCTCAGACCTGGACCCCCACCA	Mm400451
Mtap2	TTAAGGCATTTGAGCGTTGGT	CACAAGCCCATCCTAACAAAAGT	AAGAAGTGGTGTCAAAGTGCATCTCT-TAGGATTG	Mm256966
Ns1	CAACGCCCCCTTTCTTCTG	GAGCAGTCTCGTGGGAAAGC	CACCTGCTGGAAGAGGCTTGGGC	Mm331129
Ngn2	TCAGAGCTGCTGGAGGAGAAC	CCAGTTGCATTCCCTCTGAGA	CCGGGCAGGCAGTTCGTGT	Mm42017
Nr2e3	AGGCTGGAAGTTGAACAAAAGC	TCCAGTCTCCCTCCTTTCCC	AGGCACGTTTATCCTGTGTTCAAGACC-AGA	Mm103641
Nrl	AACTTCTGAGCATCGTGGCA	TGAAGAGTCGTGACCTGCAAA	CTGGTCCTTTGCTGGAGATGAGTTCCCT	Mm20422
Palm	AAAGAGCAAGAGGAACGCTTA-GG	CTCCAGCTACTGGGACATCCA	AGCCCTGCCCGGCACTCTCC	Mm253736
PCNA	TGATCCAGGGCTCCATCCT	CCCAGCAGGCCTCATTGAT	AGAAGGTGCTGGAGGCTCTCAAAGAC-CT	Mm7141
Rab27b	CCCCTGACCCCAATCTATTTTAA	GGAAGGGACTCGGGATAACAG	AAAGCAGAGTAGTCATAGTGTTGAAA-GAACTG	Mm246753
Sox-2	GAAACGACAGCTGCGGAAA	TCTAGTCGGCATCACGGTTTT	AACCACCAATCCCATCCAAATTAACG	Mm65396